**Clinical Orthopaedics
and Related Research®**
A Publication of The Association of Bone and Joint Surgeons®

Clinical Research

MRI Allows Accurate Measurement of Glenoid Bone Loss

Mirco Sgroi MD[1], Hashuka Huzurudin[1], Marius Ludwig MD[1], Timo Zippelius MD[1], Heiko Reichel MD[1],
Thomas Kappe MD[1]

Abstract

Background Bony Bankart lesions larger than a certain size can lead to a high redislocation rate, despite treatment with Bankart repair. Detection and measurement of glenoid bone loss play key roles in selecting the appropriate surgical therapy in patients with shoulder instability. There is controversy about which diagnostic modalities, using different measurement methods, provide the best diagnostic validity.

Questions/purposes (1) What are the diagnostic accuracies of true AP radiographs, West Point (WP) view radiographs, MRI, and CT to detect glenoid bone loss? (2) Are there differences in the measurements of glenoid bone loss on MRI and CT? (3) What are the intrarater and interrater reliabilities of CT and MRI to measure glenoid bone loss?

Methods Between August 2012 and February 2017, we treated 80 patients for anterior shoulder instability. Of those, we considered patients with available preoperative true AP radiographs, WP radiographs, CT images, and MR images of the affected shoulder as potentially eligible.

Based on that, 63% (50 of 80) of patients were eligible for analysis; 31% (25 of 80) were excluded because not all planes or slices (such as sagittal, axial, or frontal) of each diagnostic imaging modalities were available and 7% (5 of 80) because of the insufficient quality of diagnostic images (for example, setting of the layers did not allow adequate en face view of the glenoid). Preoperative true AP radiographs, WP radiographs, CT images and MR images of the affected shoulders were retrospectively assessed for the presence of glenoid bone loss by two blinded observers at a median (range) 25 months (12 to 66) postoperatively. To evaluate sensitivity, specificity, positive predictive value, negative predictive value, accuracy, diagnostic odds ratio, positive likelihood ratio, negative likelihood ratio, and area under the curve (AUC), we compared the detection of glenoid bone loss at follow-up achieved with the aforementioned imaging modalities with intraoperative arthroscopic detection. In all patients with glenoid bone loss, two blinded observers measured the size of the glenoid bone loss on preoperative CT and MR images using six measuring techniques: depth and length of the glenoid bone loss, Bigliani classification, best-fit circle width loss method, AP distance method, surface area method, and Gerber X ratio. Subsequently, the sizes of the glenoid bone loss determined using CT and MRI were compared. To estimate intraobserver and interobserver reliability, measurements were performed in a blinded fashion by two observers. Their level of experience was equivalent to that of orthopaedic residents, and they completed a training protocol before the measurements.

Results For the ability to accurately diagnose Bankart lesions, the AUC (accuracy of a diagnostic test; the closer to 1.0, the more accurate the test) was good for MRI (0.83 [95% confidence interval 0.70 to 0.94]; p < 0.01), fair for CT (0.79 [95% CI 0.66 to 0.92]; p < 0.01), poor for WP radiographs (0.69 [95% CI 0.54 to 0.85]; p = 0.02) and

[1]Department of Orthopaedic Surgery, Universitäts- und Rehabilitationskliniken Ulm (RKU), University of Ulm, Ulm, Germany

M. Sgroi ✉, Oberer Eselsberg 45, DE-89081 Ulm, Germany, Email: sgroi.mirco@yahoo.de

Ⓦ Wolters Kluwer

failed for true AP radiographs (0.55 [95% CI 0.39 to 0.72]; p = 0.69). In paired comparisons, there were no differences between CT and MRI regarding (median [range]) lesion width (2.33 mm [0.35 to 4.53] versus 2.26 mm [0.90 to 3.47], p = 0.71) and depth (0.42 mm [0.80 to 1.39] versus 0.40 mm [0.06 to 1.17]; p = 0.54), and there were no differences concerning the other measurement methods: best-fit circle width loss method (15.02% [2.48% to 41.59%] versus 13.38% [2.00% to 36.34%]; p = 0.66), AP distances method (15.48% [1.44% to 42.01%] versus 12.88% [1.43% to 36.34%]; p = 0.63), surface area method (14.01% [0.87% to 38.25] versus 11.72% [2.45% to 37.97%]; p = 0.68), and Gerber X ratio (0.75 [0.13 to 1.47] versus 0.76 [0.27 to 1.13]; p = 0.41). Except for the moderate interrater reliability of the Bigliani classification using CT (intraclass correlation coefficient = 0.599 [95% CI 0.246 to 0.834]; p = 0.03) and acceptable interrater reliability of the Gerber X ratio using CT (0.775 [95% CI 0.542 to 0.899]; p < 0.01), all other measurement methods had good or excellent intrarater and interrater reliabilities on MRI and CT.

Conclusion The results of this study show that CT and MRI can accurately detect glenoid bone loss, whereas WP radiographs can only recognize them poorly, and true AP radiographs do not provide any adequate diagnostic accuracy. In addition, when measuring glenoid bone loss, MRI images of the analyzed measurement methods yielded sizes that were no different from CT measurements. Finally, the use of MRI images to measure Bankart bone lesions gave good-to-excellent reliability in the present study, which was not inferior to CT findings. Considering the advantages including lower radiation exposure and the ability to assess the condition of the labrum using MRI, we believe MRI can help surgeons avoid ordering additional CT imaging in clinical practice for the diagnosis of anterior shoulder instability in patients with glenoid bone loss. Future studies should investigate the reproducibility of our results with a larger number of patients, using other measurement methods that include examination of the opposite side or with three-dimensional reconstructions.

Level of Evidence Level I diagnostic study.

Introduction

Anterior shoulder instability is common [33, 47], and making the correct diagnosis by linking patient complaints to pathologic alterations is fundamental to avoid unnecessary interventions and healthcare costs [32, 37]. Both detecting and quantifying glenoid bone loss play key roles in selecting the appropriate therapy [8, 30]. Studies have shown that glenoid bone loss larger than a certain size can lead to a high risk of redislocation, despite the use of Bankart repair [37, 41]. In these patients, bony

augmentation of the glenoid articular surface with a Latarjet procedure or iliac crest bone grafting might be considered [1, 9]. Therefore, accurate detection and quantification of glenoid bone loss can influence preoperative planning and must be accurate [30, 42]. Different imaging diagnostic modalities, including AP radiographs, West Point (WP) view radiographs, CT, and MRI are used in clinical practice to diagnose and measure the size of glenoid bone loss [6, 40]. In clinical practice, true AP radiographs are usually performed for initial shoulder evaluation, followed by special diagnostic procedures to verify the presence of bony lesions as needed.

These imaging methods' ability to accurately detect and measure glenoid bone loss is a subject of debate [3, 10, 29]. Several studies have already dealt with this topic and have investigated the clinical value of these imaging diagnostic modalities; however, contradictory results have been reported [17, 27, 46]. The diagnostic accuracy of true AP and WP radiographs, CT, and MRI in detecting glenoid bone loss remains unclear. If this study could demonstrate that one of these diagnostic procedures, such as a true AP radiograph, has no diagnostic accuracy, it should at least be discussed whether these diagnostic images and associated radiation exposure are still indicated just for this pathology. Furthermore, it would be interesting to investigate whether Bankart lesions can be measured as accurately with MRI as with CT. If so, an analysis of the intra- and interrater reliability of CT and MRI measurements should be performed [2, 23, 43]. If this study could show that MRI does not achieve lower diagnostic accuracy than CT, surgeons in clinical practice could use MRI alone to diagnose and measure glenoid bone loss, thus avoiding radiation exposure and additional costs.

Therefore, we asked: (1) What are the diagnostic accuracies of true AP radiographs, West Point (WP) view radiographs, MRI, and CT to detect glenoid bone loss? (2) Are there differences in the measurements of glenoid bone loss on MRI and CT? (3) What are the intrarater and interrater reliabilities of CT and MRI to measure glenoid bone loss?

Patients and Methods

Study Design and Setting

This was a retrospective diagnostic study comparing the relative accuracy of several imaging modalities in diagnosing glenoid bone loss against a gold standard of arthroscopic inspection and evaluating the ability of MRI in measuring glenoid bone loss against CT. It was performed at one center in Germany, and it involved two observers (HH, ML). Their level of experience was that of residents in orthopaedics.

Table 1. Demographic data of the analyzed patients (n = 50)

Parameter	Value
Women	26 (13)
Age in years	26 ± 12
Side involved, right	58 (29)
ASA classification	
ASA 1	48 (24)
ASA 2	52 (26)
ASA 3	0 (0)
ASA 4	0 (0)
BMI in kg/m^2	24.14 ± 4.17
Smokers	28 (14)

Data presented as % (n) or mean ± SD.

Participants

Between August 2012 and February 2017, we treated 80 patients for anterior shoulder instability. Of those, we considered patients with available preoperative AP radiographs, WP radiographs, CT, and MR images of the affected shoulder as potentially eligible. Based on that, 63% (50 of 80) of patients were eligible for analysis; 31% (25 of 80) were excluded because not all planes or layers (such as sagittal, axial, or frontal) of each diagnostic imaging modalities were available and 6% (5 of 80) because of the insufficient quality of diagnostic images (for example, setting of the layers did not allow adequate en face view of the glenoid).

Descriptive Data

A total of 26% (13 of 50) of patients were women. The mean age of the patients examined was 26 ± 12 years. The right side was affected in 58% (29 of 50) of patients. Twenty-eight percent (14 of 50) of patients were smokers (Table 1).

Preoperative Radiologic Setup

As part of preoperative planning and because of clinical routine, AP radiographs, WP radiographs, CT (Siemens Somatom Emotion, protocol: ST: 1.0 mm, pitch: 0.8, 130 kV), and MRI (Siemens Symphony, protocol: ST: 3.5 mm, FoV: 190 mm. Sag T2wTSE: n 28, B: 150 Hz/Px, TR: 5.750 ms, TE: 106 ms, FA: 170°; CorT1wTSE: n 28, B: 651 Hz/Px, TR: 861 ms, TE: 7.9 ms, FA: 130°; T1 axial: n 29, B: 625 Hz/Px, TR: 471 ms, TE: 8 ms, FA: 150°; T2 axial: n 29, B: 521 Hz/Px, TR: 4250 ms, TE: 98 ms, FA: 130°) of the shoulders were performed. MR images were obtained with a 1.5 Tesla MRI scanner without contrast.

Intraoperative Assessment

Arthroscopies were performed by two experienced, high-volume shoulder surgeons (MS, TK) who were not involved in the radiologic examinations. The surgical indication was based on patient history, clinical examination, and it was MRI-confirmed. All analyzed patients had clinically relevant anterior shoulder instability after at least one shoulder dislocation, and all patients were diagnosed with at least anterior labral Bankart lesion by MRI. In all patients, the decision regarding surgery was made independently from the current reporting study. All arthroscopies were performed with the patient under brachial plexus block and general anesthesia. All patients were positioned in the lateral decubitus position, and an arm-holding device (SMAR, Arthrex) was used to hold the arms. Posterior and anterolateral portals served as standard approaches. Diagnostic arthroscopy was performed. All Bankart lesions and glenoid bone losses were confirmed during diagnostic arthroscopy.

Postoperative Radiologic Analysis

Study-related radiologic analysis and measurements of the preoperative radiographs, WP radiographs, CT images, and MR images were performed in all patients at a median (range) 25 months (12 to 66) postoperatively. This was performed by two orthopaedic resident trainees (HH, ML), who analyzed and reevaluated preoperative true AP radiographs, WP radiographs, CT images, and MR images. One author (HH), who was blinded to the first measurements, took repeated measurements after at least 6 weeks. Before starting the measurements, the residents were instructed using a measurement protocol prepared by an experienced shoulder surgeon (MS). Subsequently, the residents first performed several trial measurements with patients who were not included in the study under supervision, and finally, they performed trial measurements unsupervised and repeated them after a few weeks until sufficient intrarater reliability was achieved. All measurements were performed during the same period. All imaging modalities were anonymized. All radiologic images (AP radiographs, WP radiographs, CT images, and MR images) were evaluated for the presence of glenoid bone loss. The detection of glenoid bone loss using each imaging method was then compared with intraoperative detection. To quantify the diagnostic precision of each imaging method, the following parameters were calculated: sensitivity, specificity, positive predictive value, negative predictive value, accuracy, diagnostic odds ratio, positive likelihood ratio, negative likelihood ratio, and area under the curve (AUC).

In patients who were found to have glenoid bone loss, the following measurements were performed on CT and
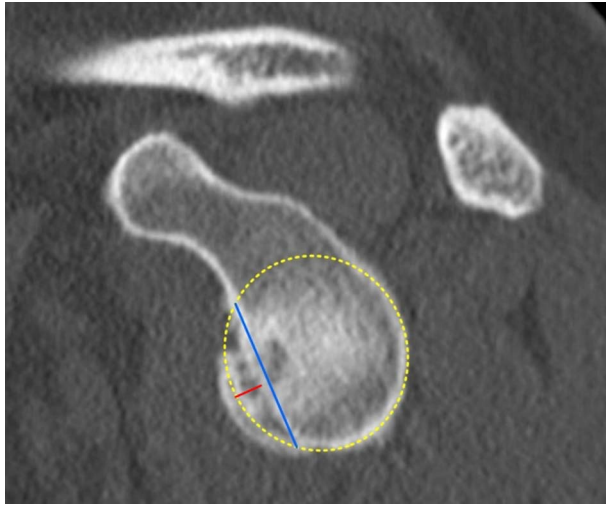
Fig. 1 This figure shows a schematic representation of the method to measure depth and length of a glenoid bone loss. A best-fit circle is placed on the lower two-thirds of the glenoid. A line connecting the anteroinferior and anterosuperior rim of the glenoid bone loss was used to measure the length of the bony defect (blue line). To measure the depth of the glenoid bone loss, a second line (red line) perpendicular to the first line was drawn between the deepest point of the glenoid bone loss and the best-fit circle. A color image accompanies the online version of this article.

MRI, in an identical manner: depth and length of the glenoid bone loss, Bigliani classification [5], best-fit circle width method [43], AP distance method [34], surface area method [44], and Gerber X ratio [40]. Measurement methods were compared between CT and MRI and not with intraoperative findings.

Depth and Length of the Bony Bankart Lesion

To measure the length and depth of the glenoid bone loss, a best-fit circle was drawn on the inferior part of the glenoid. A line connecting the anteroinferior and anterosuperior rim of the glenoid bone loss was used to measure the length of the bony defect (Fig. 1). To measure the depth of the glenoid bone loss, a second line (Fig. 1) perpendicular to the first line was drawn between the deepest point of the glenoid bone loss and the best-fit circle.

Bigliani Classification

Bigliani et al. [5] developed a classification for glenoid bone defects. According to the Bigliani classification, glenoid bone loss was classified into three categories: Type I, a displaced fracture with an attached capsule; Type II, a displaced fragment malunited to the glenoid rim; and Type

III, erosion of the glenoid rim with a defect. Because of its reproducibility and reliability [26, 45], the Bigliani classification is widespread in clinical practice and routinely used in our department, so it was included in this study.

Best-fit Circle Width Loss Method

The best-fit circle width loss method was measured as described by Sugaya et al. [44]. A best-fit circle was drawn on the inferior part of the glenoid on an en face view of the glenoid. The diameter (Fig. 2) of the best-fit circle was measured. Using a line parallel to the diameter of the best-fit circle, the width (Fig. 2) of the glenoid bone loss was measured. The amount of the involved glenoid surface was calculated by dividing the width of the glenoid bone loss by the diameter of the best-fit circle [44].

AP Distance Method

The AP distances method was performed according to Piasecki et al. [34]. After visualizing the glenoid in an en face view, we defined the bare spot. A best-fit-circle with the bare spot as the center was drawn over the inferior glenoid. The distance from the bare spot to the anterior rim and posterior rim of the glenoid was marked with a line and measured. The percentage of bone loss was calculated by dividing the distance between the bare spot and the anterior rim of the glenoid by the distance between the bare spot and
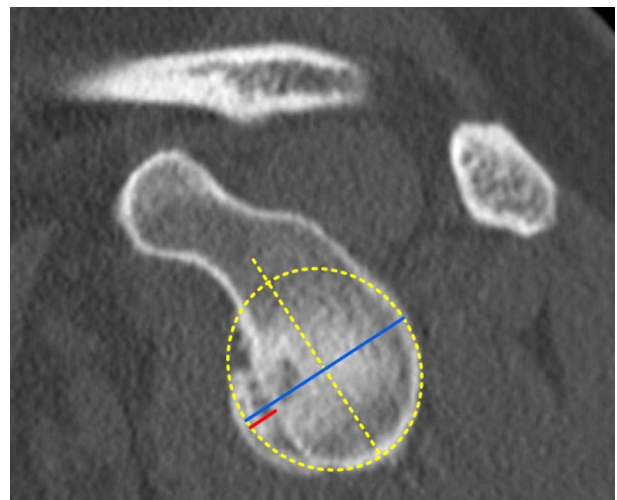

Fig. 2 This figure shows a schematic representation of the best-fit circle width loss method. A best-fit circle was drawn on the inferior part of the glenoid on an en face view of the glenoid. The diameter (blue line) of the best-fit circle was measured. Using a parallel line to the diameter of the best fit circle, the width (red line) of the glenoid bone loss was measured [39]. A color image accompanies the online version of this article.
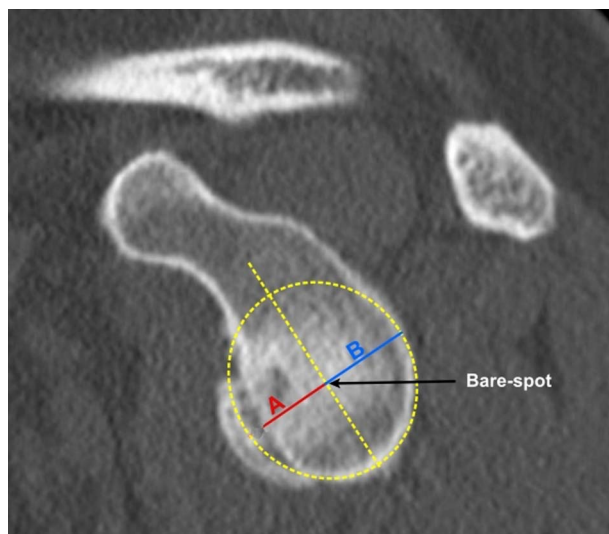
Fig. 3 This figure illustrates the AP distance method. The bare spot was identified and a best-fit circle with the bare spot as the center was drawn over the inferior glenoid. The distance A from the bare-spot area to the anterior rim of the glenoid was measured. In the same manner, the distance between the bare spot and posterior rim of the glenoid was determined. The amount of glenoidal bone loss was then calculated using the following formula: A/B x100 [32]. A color image accompanies the online version of this article.

the posterior rim of the glenoid (Fig. 3). This measurement method is frequently used (also in our department) and has been investigated in several studies with different results [28, 35, 36]. To definitively determine the actual diagnostic value, this method was included in this study.

Surface Area Method

As described by Sugaya et al. [44], a best-fit circle was first drawn from the 3 o'clock position over the lower two-thirds of the glenoid using an en face glenoid view, and its area was digitally calculated. The surface area of the bone fragment was then determined in a similar manner. The size of the glenoid bone loss was determined by dividing the area of the osseous fragment by the area of the best-fit circle (Fig. 4).

Gerber X Ratio

The Gerber X ratio was determined according to Saliken et al. [40]. Using an en face glenoid view, a best-fit circle was drawn over the lower part of the glenoid, and its diameter was measured. The length of the glenoid bone loss was measured using a line (Fig. 5) connecting the anterocranial and anterocaudal edges of the glenoid bone loss. The Gerber X ratio was calculated by dividing the length of the glenoid bone loss by the diameter of the glenoid circle

[40]. The Gerber X ratio is a highly reproducible measurement method used in our department. Despite its simple and intuitive application, this method has been little studied [42]. To validate the use of this measurement method with scientific data, it was included in this study.

The intrarater and interrater reliabilities of each measurement method using CT and MRI were calculated.

Primary and Secondary Study Outcomes

Our primary study goal was to investigate the precision of true AP radiographs, WP radiographs, MRI, and CT to detect glenoid bone loss. To achieve this, in all patients, two blinded observers (HH, ML) used all preoperative imaging modalities to evaluate the presence of glenoid bone loss at a median (range) 25 months (12 to 66) after shoulder stabilization. The detection of glenoid bone loss of each radiologic imaging method was then compared with the intraoperative detection. To calculate the diagnostic accuracy of each imaging method, we calculated different parameters for diagnostic validity.

Our secondary study goal was to analyze the diagnostic accuracy of measuring glenoid bone loss using MRI compared with the gold standard, CT. Thus, the size of the glenoid bone loss was analyzed on preoperative CT and
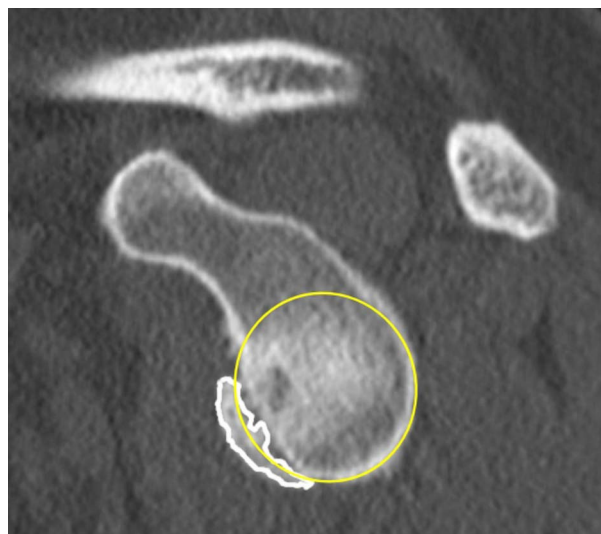
Fig. 4 This figure shows a schematic representation of the surface area measurement method. A best-fit circle is placed on the lower two-thirds of the glenoid, starting at the 3 o'clock position (yellow circle). The area of the best-fit circle was calculated digitally. The bony fragment (white line) was identified and delineated. The surface area of the bony fragment was determined digitally. The glenoid bone loss was finally calculated by determining the ratio between the two areas [39]. A color image accompanies the online version of this article.

Fig. 5 This figure shows the Gerber X ratio method. Using an en face view of the glenoid, a best-fit circle was drawn over the lower part of the glenoid, 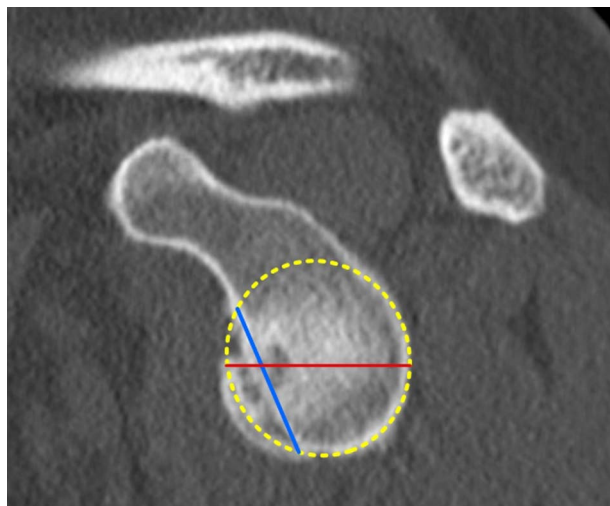and its diameter (red line) was measured. Then, the length of the glenoid bone loss was measured using a line (blue line) connecting the anterocranial and anterocaudal edges of the glenoid bone loss [34]. A color image accompanies the online version of this article.

MR images in all patients by two blinded observers (HH, ML) using different measurement methods. Then, we compared measurements of the glenoid bone loss on CT and MRI. To investigate the influence of using MRI on the measurement reliability, we also measured the intrarater and interrater reliability for each measurement.

Ethical Approval

Independent institutional review board approval was obtained from the ethics committee of the University of Ulm (number 154/20).

Statistical Analysis

The sample size calculation based on the surface area method assuming a 95% confidence interval and an effect size of 0.4, resulting in a sample size of at least 50 patients, with a power of 0.8 [16]. The sample size was sufficient to answer all three questions of the study. The statistical analysis was performed using SPSS (version 24, IBM Corp). All collected data were secured in a computerized database. Descriptive statistics were used. The accuracy for detection of glenoid bone loss was determined by comparing the imaging studies with intraoperative findings. We statistically analyzed the accuracy of each imaging modality to detect glenoid bone loss by determining the sensitivity,

specificity, positive predictive value, negative predictive value, accuracy, diagnostic odds ratio, positive likelihood ratio, negative likelihood ratio and AUC. Area under the curve is a composite measure of sensitivity and specificity originating from the receiver operating characteristic curve [19, 25]. It reflects the discriminatory accuracy of a diagnostic test and represents the mean of sensitivity for all specificities and can take a value between 0 and 1 [49]. The more relevant value for diagnostic purposes is an AUC of 0.5 because this represents the lower limit of the diagnostic validity of the analyzed test. An AUC of 0.5 means that the test under investigation is not better than chance. Conversely, the closer the AUC is to the value of 1.0, the more accurate a diagnostic test is. The AUC is context specific and cutoff values between 0.5 and 1.0 were set to define and objectively compare the quality of the different tests [12, 31, 39]: failed (0.5 to 0.6), poor (0.6 to 0.7), fair (0.7 to 0.8), good (0.8 to 0.9), and excellent (0.9 to 1.0) [18, 39]. The Yates chi-square test was used to compare each imaging modality's findings with the intraoperative findings. The results of each measurement method performed on MRI were compared with those performed on CT to determine each measurement method's ability to quantify the dimension of the detected osseous Bankart lesion, depending on the imaging modality. When comparing measurement methods between CT and MRI, two measurements were performed in a pairwise comparison for one group. Therefore, the Wilcoxon signed-rank test and the sign test were used as t-tests for interval-scaled parameters and ordinal-scaled dimensions, respectively. To obtain intrarater and interrater correlations, two orthopaedic surgeons (HH, ML) repeated all measurements; one of them (HH), who was blinded to the first measurements, took repeated measurements after at least 6 weeks. The intrarater reliability was evaluated with the chi-square test for nominal scaled measurements, Spearman rank correlation coefficient for ordinal scaled measurements, and the Pearson correlation coefficient for interval-scaled measurements. The interrater reliability was calculated using the intraclass correlation coefficient. Intraclass correlation coefficient reflects the degree of consistency between measurements made by different observers [48]. Intrarater and interrater correlation coefficients are generally interpreted as follows: ≤ 0.5 were considered poor, between 0.5 and 0.75 were classified as moderate, between 0.75 and 0.90 were good, and > 0.90 were deemed excellent [13, 22]. Despite this interpretation, it should be kept in mind that an intraclass correlation coefficient of 0.75 means that a significant percentage of the measurements are not consistent. On the other hand, it should be noted that the intraclass correlation does not reflect the correctness of the performed measurement methods. Thus, if all three observers measure incorrectly in a similar way, there results still have a high intraclass correlation. The intraclass correlation does not describe the quality of the

Table 2. Diagnostic validity of AP radiographs, WP radiographs, CT, and MRI compared with intraoperative findings (n = 50)

	AP (95% CI)	WP (95% CI)	CT (95% CI)	MRI (95% CI)
Sensitivity	0.44 (0.21-0.69)	0.67 (0.41-0.86)	0.89 (0.65-0.98)	0.94 (0.71-0.99)
Specificity	0.65 (0.46-0.81)	0.72 (0.53-0.86)	0.69 (0.50-0.83)	0.63 (0.45-0.80)
PPV	0.42 (0.26-0.59)	0.57 (0.41-0.71)	0.61 (0.48-0.73)	0.59 (0.47-0.70)
NPV	0.68 (0.56-0.77)	0.79 (0.65-0.88)	0.91 (0.74-0.97)	0.95 (0.74-0.99)
Accuracy	0.58 (0.43-0.72)	0.70 (0.55-0.82)	0.76 (0.61-0.86)	0.74 (0.60-0.86)
DOR	1.53 (0.46-4.97)	5.12 (1.46-17.78)	17.60 (3.38-91.56)	27.6 (3.21-237.83)
LR +	1.26 (0.64-2.61)	2.40 (1.25-4.51)	2.87 (1.66-4.88)	2.54 (1.63-4.33)
LR -	0.86 (0.52-1.37)	0.46 (0.23-0.92)	0.16 (0.04-0.61)	0.09 (0.01-0.62)
AUC	0.55 (0.39-0.72)	0.69 (0.54-0.85)	0.79 (0.66-0.92)	0.83 (0.70-0.94)
p value[a]	0.69	0.02	< 0.001	< 0.001
Cramer V	0.48 (p = 0.10)	0. 37 (p < 0.01)	0.55 (p < 0.01)	0.67 (p < 0.01)

[a]The p values represent the comparison of each imaging modality (AP, WP, CT, and MRI) against the arthroscopic findings; the Cramer V test describes the strength of the correlation between the results of each diagnostic imaging against arthroscopic findings; WP = West Point; PPV = positive predictive value; NPV = negative predictive value; DOR = diagnostic odds ratio; LR + = positive likelihood ratio; LR- = negative likelihood ratio; AUC = area under the curve.

diagnostic test but the internal consistency of a measurement [22]. Differences were considered significant for p values < 0.05.

Results

Diagnostic Accuracy for Detecting Bankart Lesions

For the ability to accurately diagnose Bankart lesions, the AUC was good for MRI (0.83 [95% CI 0.70 to 0.94]; p < 0.001), fair for CT (0.79 [95% CI 0.66 to 0.92]; p < 0.001), poor for WP radiographs (0.69 [95% CI 0.54 to 0.85]; p = 0.02), and failed for true AP radiographs (0.55 [95% CI 0.39 to 72]; p = 0.69) (Table 2).

CT and MRI Measurements of Bankart Lesions

In paired comparisons, there were no differences in the median (range) width of lesions between CT and MRI (2.33 mm [0.35 to 4.53] versus 2.26 mm [0.90 to 3.47], mean difference 0.07 mm; p = 0.71) and depth (0.42 mm [0.80 to 1.39] versus 0.40 mm [0.06 to 1.17], mean difference 0.02 mm; p = 0.54), and there were no differences in the other measurements methods: Bigliani classification (1.50 [1.00 to 2.00] versus 2.00 [1.00 to 3.00], mean difference 0.50; p = 0.33); best-fit circle width loss method (15.02% [2.48% to 41.59%] versus 13.38% [2.00% to 36.34%], mean difference 1.64%; p = 0.66), AP distances method (15.48% [1.44% to 42.01%] versus 12.88% [1.43% to 36.34%], mean difference 2.60%; p = 0.63), surface area method (14.01% [0.87% to 38.25%] versus 11.72% [2.45% to 37.97%], mean difference 2.29%; p =

0.68), and Gerber X ratio (0.75 [0.13 to 1.47] versus 0.76 [0.27 to 1.13], mean difference 0.01; p = 0.41) (Table 3).

Intrarater and Interrater Reliabilities of CT and MRI

In this study, except for the moderate interrater reliability of the Bigliani classification performed using CT (intraclass correlation coefficient = 0.599 [95% CI 0.246 to 0.834]; p = 0.03) and good interrater reliability using CT of the Gerber X ratio (0.775 [95% CI 0.542 to 0.899]; p < 0.01), the intrarater and interrater reliabilities were excellent for all measurements, irrespective of the imaging modality. The intrarater (Table 4) and interrater reliabilities (Table 5) of the other measuring methods using CT and MRI were: for the AP distances method 0.964 (95% CI 0.927 to 0.984; p < 0.01) versus 0.903 (95% CI 0.799 to 0.958; p < 0.01), for the surface area method 0.959 (95% CI 0.917 to 0.982; p < 0.01) versus 0.884 (95% CI 0.765 to 0.984; p < 0.01), and for the Gerber X ratio 0.775 (95% CI 0.542 to 0.899; p < 0.01) versus 0.871 (95% CI 0.738 to 0.942; p < 0.01) (Table 5).

Discussion

Studies have shown that the accurate detection and measurement of glenoid bone loss is crucial for the appropriate choice of surgical approach in patients with shoulder instability [29, 31]. However, it is still unclear which diagnostic modalities have the best validity and with which measurement methods. This analysis showed that in detecting glenoid bone loss, CT and MRI were accurate, WP radiographs were poor, and AP radiographs were not

Table 3. Comparison of measurement methods between MRI and CT

	CT	MRI	Difference of medians	p value
Width in cm	2.33 (0.35-4.53)	2.26 (0.90-3.47)	0.07	0.71
Depth in cm	0.42 (0.80-1.39)	0.40 (0.06-1.17)	0.02	0.54
Bigliani classification in °	1.50 (1.00-2.00)	2.00 (1.00-3.00)	0.50	0.33
Best-fit circle width, %	15.02 (2.48-41.59)	13.38 (2.00-36.34)	1.64	0.66
AP distances, %	15.48 (1.44-42.01)	12.88 (1.43-36.34)	2.60	0.63
Surface area, %	14.01 (0.87-38.25)	11.72 (2.45-37.97)	2.29	0.68
Gerber X ratio	0.75 (0.13-1.47)	0.76 (0.27-1.13)	0.01	0.41

Data presented as the median (range); the results of each measurement were not normally distributed; the Wilcoxon signed-rank test was used to compare the interval scaled measurements; ordinal scaled variables were tested with the sign test.

adequate at all. In addition, there were no differences in diagnostic accuracy and reliability between CT and MRI in measuring glenoid bone loss with the investigated measurement methods. Considering the results of the present study and the fact that MRI avoids radiation exposure and allows assessment of the condition of the labrum, it can be suggested that MRI can be safely used in clinical practice to diagnose anterior shoulder instability even in patients with glenoid bone loss.

Limitations

The current study has several limitations. First, it included a limited number of patients. In the present study, a highly selected group of patients was included, namely only patients who had an indication for surgical intervention. This may have influenced the specificity of the present study because the number of true negative patients probably remained small due to the preselection. On the other hand, in the present study, the entire spectrum of patients with anterior shoulder instability was considered regardless of the degree of instability, including patients with suspected glenoid bone loss. The aim of the present study was not to investigate the diagnostic accuracy in diagnosing anterior

shoulder instability per se but to investigate the ability of different imaging modalities to identify patients with glenoid bone loss among all patients with anterior shoulder instability. Shoulder surgeons frequently encounter this problem preoperatively; therefore, given their relevance and concordance with the clinical practice, the included patient population seems to be appropriate. Second, the bone defect measurements obtained with the imaging procedures were not compared with arthroscopically estimated values. This study was a retrospective one. Different surgeons operated on the patients, which means that the arthroscopic measurements were performed in different settings and with various techniques. A comparison with the size of the bone defect measured directly intraoperatively may seem more appropriate. However, this is only partially true because the measurement methods included in the study were developed exclusively for use in imaging procedures. Intraoperative application of all other included measurement methods would not be validated and might be difficult due to the different setting and angle of view. Third, no comparison with the contralateral uninjured side was performed. Several studies have developed measurement methods based on a comparison with the contralateral healthy side [27, 40]. In clinical practice, we use measurement methods based exclusively on the

Table 4. Intrarater reliability of measurements with CT and MRI

Variable	CT (95% CI)	p value	MRI (95% CI)	p value
Width	0.921 (0.809-0.987)	< 0.01	0.901 (0.807-0.989)	< 0.01
Depth	0.964 (0.895-0.995)	< 0.01	0.965 (0.898-0.994)	< 0.01
Bigliani	0.895 (0.731-1.000)	< 0.01	0.951 (0.882-0.999)	< 0.01
Best-fit circle width	0.981 (0.952-0.996)	< 0.01	0.964 (0.890-0.994)	< 0.01
AP distances	0.990 (0.973-0.997)	< 0.01	0.982 (0.961-0.994)	< 0.01
Surface area	0.979 (0.929-0.996)	< 0.01	0.985 (0.940-0.999)	< 0.01
Gerber X ratio	0.900 (0.743-9.83)	< 0.01	0.854 (0.631-0.998)	< 0.01

The correlation of nominal scaled measurements was compared using the chi-square test, ordinal scaled measurements were compared using the Spearman rank correlation coefficient, and interval scaled measurements were compared using the Pearson correlation coefficient.

Table 5. Interrater reliability of measurements with CT and MRI

Variable	CT (95% CI)	p value	MRI (95% CI)	p value
Width	0.846 (0.664-0.937)	< 0.01	0.951 (0.871-0.985)	< 0.01
Depth	0.925 (0.792-0.978)	< 0.01	0.958 (0.878-0.989)	< 0.01
Bigliani	0.599 (0.246-0.834)	0.02	0.834 (0.650-0.922)	< 0.01
Best-fit circle width	0.898 (0.731-0.968)	< 0.01	0.953 (0.887-0.985)	< 0.01
AP distances	0.964 (0.927-0.984)	< 0.01	0.903 (0.799-0.958)	< 0.01
Surface area	0.959 (0.917-0.982)	< 0.01	0.884 (0.765-0.984)	< 0.01
Gerber X ratio	0.775 (0.542-0.899)	< 0.01	0.871 (0.738-0.942)	< 0.01

The interrater reliability was measured using the intraclass correlation coefficient.

affected side. A comparison with the contralateral side is associated with higher radiation exposure for CT and higher cost and time for MRI. It is also not clearly demonstrated that methods comparing the affected side with the unaffected side have higher accuracy [7, 40]. Fourth, we did not consider any three-dimensional (3D) imaging methods; had they been used, they may have been helpful in examining the concave shape of the glenoidal cavity. Nevertheless, several studies on this topic have been conducted [4, 6, 17], and a definitive advantage of the 3D technique over two-dimensional (2D) imaging has not been demonstrated. Additionally, not all clinics can perform 3D reconstruction. On the other hand, it should be noted that when using 2D images, there may be errors in the primary reconstruction of the sagittal en face view if the axial image has not been set up correctly. Fifth, because this was a retrospective study, specific a priori standardization of imaging techniques was not possible. This is, of course, a limitation of the present study. This applies to the radiographs as well as to the CT and MRI images. Particularly for the CT and MRI images, the correct image formatting is important for the setting of the en face view. However, the selection of included patients was based on the formatting and setting of the images in advance, and patients whose image quality was not adequate were excluded. Sixth, radiographic analysis did not include other imaging modalities that are often part of a standard shoulder series (such as, scapular Y views, axillary views, Grashey views, or AP views in internal or external rotation). Thus, the present study cannot definitively answer whether the included imaging methods are better than other commonly used methods. Since our study is retrospective, this aspect could not be influenced. Furthermore, it should be considered that the inclusion of additional radiological modalities would have increased the radiation exposure of the patients, which is not justifiable for ethical reasons. Seventh, we used a 1.5 Tesla and not a 3.0 Tesla MRI because we only have a 1.5 Tesla MRI in our clinic. A 3.0 Tesla MRI would have further improved the accuracy of the diagnostic measurement methods analyzed because of better resolution. This might have further highlighted the advantages of MRI over CT. On the other hand, it should be considered that not all clinics have the capability to use a 3.0 Tesla MRI. Therefore, the use of a 3.0 Tesla MRI may have limited the translational significance of the study. Eighth, we did not include patients with MR arthrograms. This might have improved the analysis of the soft tissue labral structures. However, because the focus of the present study was on the bony Bankart lesions, the use of MR arthrograms would not have impacted the results. Finally, in our study, only one of the two observers repeated the measurements. Both observers underwent trial training before the start of measurements, during which several trial measurements took place after verbal and written instruction. The observers started real measurements only when the respective intrarater reliabilities were good. Additional repetition of measurements by the second observer would therefore probably not have had a significant effect on data validity.

Detection of Bony Bankart Lesions With True AP Radiographs, WP Radiographs, MRI, and CT

In our study, CT and MRI accurately diagnosed glenoid bone loss, and WP radiographs demonstrated poor diagnostic accuracy; true AP radiographs, on the other hand, failed diagnostic accuracy. The diagnostic validity of true AP and WP radiographs had been sparsely investigated [21]. One study used radiographs to analyze the prevalence of glenoid bone loss accompanying chronic anterior shoulder instability and found an incidence of glenoid bone loss of 8.2% on AP radiographs [11]. Another study compared the diagnostic reliability of radiographs, CT, and MRI in seven pairs of human cadaveric shoulders [38]. In one other study, AP radiographs were shown to achieve poor results [6]. In a biomechanical study by Itoi et al. [20] with 12 cadaveric scapulae, bone defects of 0%, 9%, 21%, 34%, and 46% of the glenoid surface were generated, and WP radiographs and CT images were obtained. The authors of that study found that a 21% defect corresponds to 18.6% of an intact glenoid on WP radiographs. In contrast, for CT, a 21% defect resulted in a loss of 50% of the width

of the lower quarter of the glenoid. The authors concluded that glenoid defect size could be accurately estimated using WP radiographs or CT. Considering the different study designs, the results of the current study extend and complement the conclusions by the studies discussed here. Based on the results of our study, WP radiographs appear to be a screening method with poor but sufficient accuracy in detecting glenoid bone loss. WP radiographs can therefore only be recommended as a screening method, but because of their poor accuracy, they should only be used as a supplement and not as substitute for CT or MRI. On the other hand, there is no scientific support for the use of AP radiographs for glenoid bone loss detection in daily clinical practice.

Several studies have examined the accuracy of CT imaging and MRI in detecting osseous Bankart lesions, sometimes with contradictory results [4, 7, 27]. For instance, one study compared CT and arthroscopy for detecting glenoid bone loss in 50 patients and found that CT had a sensitivity and specificity of 97.2% and 77.8%, respectively [15]. Conversely, another study investigated the agreement among MRI, CT, and arthroscopy for measuring glenoid bone loss in 176 patients [23]. In this study, MRI assessment of glenoid bone loss proved to be almost as accurate as CT assessment [24]. A further study compared the value of 3D CT imaging and MRI for surgical planning in recurrent anterior shoulder instability in a study of 83 patients; MRI had low sensitivity, whereas CT imaging provided an accurate prediction of intraoperative findings [29]. We found that CT and MRI did not differ in terms of sensitivity and specificity in detecting glenoid bone loss. However, MRI revealed a higher area under the curve and a stronger concordance with arthroscopic findings. Consequently, MRI could be considered a valid option in clinical practice for the diagnosis of anterior shoulder instability in patients with glenoid bone loss. If one additionally considers that MRI can reduce radiation exposure and allow the detection and evaluation of labral disease compared with CT, MRI can help to avoid needing to order additional CT imaging to obtain glenoidal defect size for surgical plaining. Before that, however, further studies are needed to confirm the results of the current study.

Accuracy and Reliability of Measurement of Bony Bankart Lesions Using MRI Compared With CT

We found that all measurement methods analyzed in the current study can be performed on both MRI and CT images without significant loss of diagnostic accuracy. Bigliani et al. [5] developed the Bigliani classification and found that 76% of glenoid bone defects were correctly identified on plain radiographs and that all defects could be correctly identified and classified with the CT arthrogram. The best-fit circle width loss method and AP distance

method have been investigated, with contradictory results [24, 29]. For instance, in a study with 65 patients, the validity of the best-fit circle width loss method was assessed to quantify glenoid bone loss using MRI against CT and arthroscopy; this study found that MRI imaging evaluation of glenoid bone loss using the best-fit circle width loss method is nearly as accurate as CT [24]. Regarding the Bigliani classification, there was no statistical difference between CT and MRI in terms of classification grading in the current study; however, CT was found to have moderate interrater reliability. In the present study, the AP distances and best-fit circle width loss method showed few differences between measurements performed with CT and those performed with MRI; however, these differences were not statistically relevant. Considering the results of the present study, the use of these measurement methods with MRI can be recommended without statistically significant reduction in accuracy compared with CT.

Some studies have considered the diagnostic validity of the surface area method using the ipsilateral shoulder [17, 24, 29]. A retrospective study analyzed the surface area method in 48 patients with recurrent anterior shoulder instability using CT and MRI; CT enabled a more accurate estimation of glenoid bone loss than MRI [29]. Conversely, Tian et al. [46] used CT and MRI and compared measurements of glenoid bone loss using the surface area method in 41 patients, and they found excellent reliability. In the current study, measurements of glenoid bone loss with the surface area method demonstrated identical accuracy between CT and MRI. Nevertheless, when this measurement method was performed on CT images, slightly higher interrater reliability was achieved. The results of this study suggest that the surface area method is an accurate way to assess glenoid bone loss with CT and MRI, although MRI tends to have a slightly lower interrater correlation because of the overlay of soft tissue.

The Gerber X ratio's ability to measure glenoid bone loss has rarely been investigated [14, 42]. One study analyzed the value of the Gerber X ratio in 77 patients with anterior shoulder instability and concluded that the Gerber X ratio was a reproducible method for assessing glenoid bone loss [42]. In the present study, the Gerber X ratio method had almost identical results on CT and MRI. The intrarater and interrater reliabilities both were good or excellent, with MRI having higher interrater reliability. The use of MRI to measure glenoid bone loss using the Gerber X ratio is fully supported by the results of the present study and can therefore be recommended.

Conclusion

The present study showed that CT and MRI can accurately detect glenoid bone loss, whereas WP radiographs can only

recognize them poorly, and AP radiographs do not provide any adequate diagnostic accuracy. Moreover, the current study confirmed that regarding the measurement of glenoid bone loss, the analyzed measuring methods can be performed using MRI, yielding results that were not different from those obtained with CT. Regarding intrarater and interrater reliabilities, all measurement techniques, except for the interrater reliability of the Bigliani classification on CT, showed good or excellent reliabilities with CT and MRI. Considering the results of our study and because MRI avoids radiation exposure and allows the evaluation of concomitant labral pathologies compared with CT, MRI should be considered a valid option for the diagnosis of glenoid bone loss in clinical practice. An additional advantage of MRI may be that shoulder surgeons do not need to order a dedicated CT to get measurements of glenoid bone loss. However, the results of the present study must be confirmed by further research. Future studies should evaluate the reproducibility of our results in terms of the diagnostic accuracy of MRI compared with other measurement methods, possibly including 3D-CT or measurement methods involving the contralateral side.

References

1. Ali ZS, Hurley ET, Jamal MS, et al. Low rate of recurrent instability following the open Latarjet procedure as a revision procedure for failed prior stabilization surgery. *Knee Surg Sports Traumatol Arthrosc*. 2021;29:2110-2117.
2. Altan E, Ozbaydar MU, Tonbul M, Yalcin L. Comparison of two different measurement methods to determine glenoid bone defects: area or width? *J Shoulder Elbow Surg*. 2014;23: 1215-1222.
3. Auffarth A, Mayer M, Kofler B, et al. The interobserver reliability in diagnosing osseous lesions after first-time anterior shoulder dislocation comparing plain radiographs with computed tomography scans. *J Shoulder Elbow Surg*. 2013;22:1507-1513.
4. Bakshi NK, Patel I, Jacobson JA, Debski RE, Sekiya JK. Comparison of 3-dimensional computed tomography-based measurement of glenoid bone loss with arthroscopic defect size estimation in patients with anterior shoulder instability. *Arthroscopy*. 2015;31:1880-1885.
5. LU Bigliani, Newton PM, Steinmann SP, Connor PM, McIlveen SJ. Glenoid rim lesions associated with recurrent anterior dislocation of the shoulder. *Am J Sports Med*. 1998;26:41-45.
6. Bishop JY, Jones GL, Rerko MA, Donaldson C, MOON Shoulder Group. 3-D CT is the most reliable imaging modality when quantifying glenoid bone loss. *Clin Orthop Relat Res*. 2013;471:1251-1256.
7. Bois AJ, Fening SD, Polster J, Jones MH, Miniaci A. Quantifying glenoid bone loss in anterior shoulder instability: reliability and accuracy of 2-dimensional and 3-dimensional computed tomography measurement techniques. *Am J Sports Med*. 2012;40:2569-2577.
8. Burkhart SS, Danaceau SM. Articular arc length mismatch as a cause of failed bankart repair. *Arthroscopy*. 2000;16:740-744.
9. Burkhart SS, De Beer JF, Barth JRH, et al. Results of modified Latarjet reconstruction in patients with anteroinferior instability and significant bone loss. *Arthroscopy*. 2007;23:1033-1041.
10. Charousset C, Beauthier V, Bellaïche L, et al. Can we improve radiological analysis of osseous lesions in chronic anterior shoulder instability? *Orthop Traumatol Surg Res*. 2010;96: S88-93.
11. Edwards TB, Boulahia A, Walch G. Radiographic analysis of bone defects in chronic anterior shoulder instability. *Arthroscopy*. 2003;19:732-739.
12. El Khouli RH, Macura KJ, Barker PB, et al. The relationship of temporal resolution to diagnostic performance for dynamic contrast enhanced (DCE) MRI of the breast. *J Magn Reson Imaging*. 2009;30:999-1004.
13. Enderlein G, Fleiss JL. The design and analysis of clinical experiments. *Biometrical Journal*. 1988;30:304-304.
14. Gerber C, Nyffeler RW. Classification of glenohumeral joint instability. *Clin Orthop Relat Res*. 2002;400:65-76.
15. Griffith JF, Yung PSH, Antonio GE, Tsang PH, Ahuja AT, Chan KM. CT compared with arthroscopy in quantifying glenoid bone loss. *AJR Am J Roentgenol*. 2007;189:1490-1493.
16. Guyatt GH, Mills EJ, Elbourne D. In the era of systematic reviews, does the size of an individual trial still matter? *PLoS Med*. 2008;5:e4.
17. Gyftopoulos S, Hasan S, Bencardino J, et al. Diagnostic accuracy of MRI in the measurement of glenoid bone loss. *AJR Am J Roentgenol*. 2012;199:873-878.
18. Hanley JA, McNeil BJ. The meaning and use of the area under a receiver operating characteristic (ROC) curve. *Radiology*. 1982; 143:29-36.
19. Hosmer DW Jr, Lemeshow S, Sturdivant RX. *Applied Logistic Regression*. John Wiley & Sons; 2013.
20. Itoi E, Lee S-B, Amrami KK, Wenger DE, An K-N. Quantitative assessment of classic anteroinferior bony Bankart lesions by radiography and computed tomography. *Am J Sports Med*. 2003; 31:112-118.
21. Itoi E, Lee SB, Berglund LJ, Berge LL, An KN. The effect of a glenoid defect on anteroinferior stability of the shoulder after Bankart repair: a cadaveric study. *J Bone Joint Surg Am*. 2000; 82:35-46.
22. Koo TK, Li MY. A guideline of selecting and reporting intraclass correlation coefficients for reliability research. *J Chiropr Med*. 2016;15:155-163.
23. Lacheta L, Herbst E, Voss A, et al. Insufficient consensus regarding circle size and bone loss width using the ratio-"best fit circle"-method even with three-dimensional computed tomography. *Knee Surg Sports Traumatol Arthrosc*. 2019;27: 3222-3229.
24. Lee RKL, Griffith JF, Tong MMP, Sharma N, Yung P. Glenoid bone loss: assessment with MR imaging. *Radiology*. 2013;267:496-502.
25. Mandrekar JN. Receiver operating characteristic curve in diagnostic test assessment. *J Thorac Oncol*. 2010;5:1315-1316.
26. Martetschläger F, Kraus TM, Hardy P, Millett PJ. Arthroscopic management of anterior shoulder instability with glenoid bone defects. *Knee Surg Sports Traumatol Arthrosc*. 2013;21:2867-2876.
27. Milano G, Saccomanno MF, Magarelli N, Bonomo L. Analysis of agreement between computed tomography measurements of glenoid bone defects in anterior shoulder instability with and without comparison with the contralateral shoulder. *Am J Sports Med*. 2015;43:2918-2926.
28. Miyatake K, Takeda Y, Fujii K, Takasago T, Iwame T. Validity of arthroscopic measurement of glenoid bone loss using the bare spot. *Open Access J Sports Med*. 2014;5:37-42.
29. Moroder P, Resch H, Schnaitmann S, Hoffelner T, Tauber M. The importance of CT for the pre-operative surgical planning in recurrent anterior shoulder instability. *Arch Orthop Trauma Surg*. 2013;133:219-226.

30. Nakagawa S, Mae T, Yoneda K, Kinugasa K, Nakamura H. Influence of glenoid defect size and bone fragment size on the clinical outcome after arthroscopic Bankart repair in male collision/contact athletes. *Am J Sports Med.* 2017;45:1967-1974.

31. Obuchowski NA. Receiver operating characteristic curves and their use in radiology. *Radiology.* 2003;229:3-8.

32. Owens BD, Campbell SE, Cameron KL. Risk factors for anterior glenohumeral instability. *Am J Sports Med.* 2014;42:2591-2596.

33. Owens BD, Duffey ML, Nelson BJ, DeBerardino TM, Taylor DC, Mountcastle SB. The incidence and characteristics of shoulder instability at the United States Military Academy. *Am J Sports Med.* 2007;35:1168-1173.

34. Piasecki DP, Verma NN, Romeo AA, Levine WN, Bach BR, Provencher MT. Glenoid bone deficiency in recurrent anterior shoulder instability: diagnosis and management. *J Am Acad Orthop Surg.* 2009;17:482-493.

35. Ramos MRF, Hidalgo PF, Fagundes D, San YAC. Bare spot location in glenoid cavity: comparison between arthroscopy and CT scan. *Acta Ortop Bras.* 2020;28:243-246.

36. Ramos MRF, San Junior YAC, Alves LHP, Cruz FC, Mansur H. Is the bare spot reliable for the bone loss measurement? *Shoulder Elbow.* 2019;11:106-112.

37. Randelli P, Ragone V, Carminati S, Cabitza P. Risk factors for recurrence after Bankart repair a systematic review. *Knee Surg Sports Traumatol Arthrosc.* 2012;20:2129-2138.

38. Rerko MA, Pan X, Donaldson C, Jones GL, Bishop JY. Comparison of various imaging techniques to quantify glenoid bone loss in shoulder instability. *J Shoulder Elbow Surg.* 2013; 22:528-534.

39. Safari S, Baratloo A, Elfil M, Negida A. Evidence based emergency medicine; part 5 receiver operating curve and area under the curve. *Emerg (Tehran).* 2016;4:111-113.

40. Saliken DJ, Bornes TD, Bouliane MJ, Sheps DM, Beaupre LA. Imaging methods for quantifying glenoid and Hill-Sachs bone loss in traumatic instability of the shoulder: a scoping review. *BMC Musculoskelet Disord.* 2015;16:164.

41. Salomonsson B, von Heine A, Dahlborn M, et al. Bony Bankart is a positive predictive factor after primary shoulder dislocation. *Knee Surg Sports Traumatol Arthrosc.* 2010;18:1425-1431.

42. Sommaire C, Penz C, Clavert P, Klouche S, Hardy P, Kempf JF. Recurrence after arthroscopic Bankart repair: is quantitative radiological analysis of bone loss of any predictive value? *Orthop Traumatol Surg Res.* 2012;98:514-519.

43. Sugaya H. Techniques to evaluate glenoid bone loss. *Curr Rev Musculoskelet Med.* 2014;7:1-5.

44. Sugaya H, Moriishi J, Dohi M, Kon Y, Tsuchiya A. Glenoid rim morphology in recurrent anterior glenohumeral instability. *J Bone Joint Surg Am.* 2003;85:878-884.

45. Tennent DJ, Donohue MA, Posner MA. Bone loss and glenohumeral instability. *Sports Med Arthrosc Rev.* 2017;25: 131-135.

46. Tian C-Y, Shang Y, Zheng Z-Z. Glenoid bone lesions: comparison between 3D VIBE images in MR arthrography and nonarthrographic MSCT. *J Magn Reson Imaging.* 2012;36: 231-236.

47. Trojan JD, Meyer LE, Edgar CM, Brown SM, Mulcahey MK. Epidemiology of shoulder instability injuries in collision collegiate sports from 2009 to 2014. *Arthroscopy.* 2020;36:36-43.

48. Ursachi G, Horodnic IA, Zait A. How reliable are measurement scales? External factors with indirect influence on reliability estimators. *Procedia Economics and Finance.* 2015; 20:679-686.

49. Zhou X-H, McClish DK, Obuchowski NA. *Statistical Methods in Diagnostic Medicine.* John Wiley & Sons; 2009.